International Journal of Engineering Sciences &Research Technology

(A Peer Reviewed Online Journal)
Impact Factor: 5.164

IJESRT

RESEARCHERID
THOMSON REUTERS

ISSN: 2277-9655
[KODJO, *et al.*, 8(10): October, 2019] Impact Factor: 5.164
IC™ Value: 3.00 CODEN: IJESS7

IJESRT

INTERNATIONAL JOURNAL OF ENGINEERING SCIENCES & RESEARCH TECHNOLOGY

DYNAMIC EVALUATION OF GLOBAL SOLAR POTENTIAL IN THE REGION OF KARA (TOGO) BY ARTIFICIAL NEURAL NETWORK

Serge Dzo Mawuefa AFENYIVEH[1], KoffiMawugno KODJO[*2] & Hoavo HOVA[1]

[1]Laboratory Materials, Renewable Energies and Environment, Department of Physics, University of Kara, Kara, Togo

[*2]Research Laboratory in Engineering Sciences, Department of Electrical Engineering, University of Lomé, Lomé, Togo

DOI: 10.5281/zenodo.3523008

ABSTRACT

In this paper, a Multilayer Perceptron model of Artificial Neural Networks with a Levenberg-Marquardt learning algorithm is designed for the prediction of solar potential in the region of Kara. For the most efficient architecture after learning, the correlation coefficient (R) and the Root Mean Square Error (RMSE) are respectively 0.84902 and 0.4000. In order to determine the model of the network to be used for the prediction, the number of neurons in the hidden layer as well as the couples of transfer functions are varied. The best results at the end of the prediction are obtained with an architecture which activation function pair is Tansig-Purelin and three (03) neurons under the hidden layer. The quality of the results obtained is satisfactory. It provides a powerful model for day-to-day prediction.

KEYWORDS: Global solar radiation, Artificial Neural Networks, Multilayer Perceptron.

1. INTRODUCTION

Knowledge of the solar energy resource is a prerequisite for the proper sizing of photovoltaic conversion systems and the choice of their location. However, solar radiation is one of the most difficult meteorological parameters to estimate because it is a function of several geographical and astronomical parameters and is dependent on meteorological and atmospheric conditions [1]. In fact, the spatio-temporal variation of solar radiation is a major factor in the design of photovoltaic conversion systems and consequently in the power produced by the conversion system. In other words, to resort to alternative energies in case of unavailability of solar energy and therefore to have electrical energy in a sustainable manner, the prediction is essential. It allows better use of solar renewable energy which intermittence heavily penalizes its use.

Indeed, there are many models to make a prediction of time series. It is possible to group them into four large groups. We distinguish "naive" models, which are essential for verifying the validity of complex models (persistence, mean or k-nearest neighbors); conditional probability models rarely mentioned in the literature with regard to global solar radiation (Markov chains and predictions based on Bayesian inferences); the reference models by the number of studies that have used them, which come from the large family of seasonal autoregressive moving average models (SARIMA) and lastly connectionist-type models (artificial neural network), more particularly the multilayer perceptron, which is a type of neural networks with high predictive potential and most often used [2], [3].

On the one hand, artificial neural networks have attracted the attention of a large number of researchers in the field of renewable energies, and in particular for the prediction of meteorological data such as solar radiation [1]. Also, much research has proven the ability of neural networks to predict weather data. They have shown that they are more appropriate and give better results compared to conventional approximation methods proposed by other researchers forthe prediction of solar radiation [4],[5].

The region of Kara has a very favorable climate for the use of solar energy, especially solar photovoltaic (the rate of sunshine is around 2700h / year [6]).However, the optimal use of this source for the design of solar

ISSN: 2277-9655
Impact Factor: 5.164
CODEN: IJESS7

photovoltaic systems faces the major challenge of the intermittent nature of solar radiation. The aim of this study is to develop several predictive neuronal models of global mean solar radiation received on a horizontal plane in the region of Kara in order to choose the best performing model for its prediction.

2. MATERIALS AND METHODS

This section is devoted initially to the description of the site of the study and then to the data used.

General characteristics of the site

Located in the northern part of Togo (400 km north of the capital Lomé), the regional area of Kara is made up of seven (07) prefectures covering an area of 11738 km^2, nearly 21% of the national territory[7]. With a population of 769940 inhabitants at the last general census of population and housing [8] the Kara region is the fourth most populous region of the five administrative regions of Togo (see Figure 1).

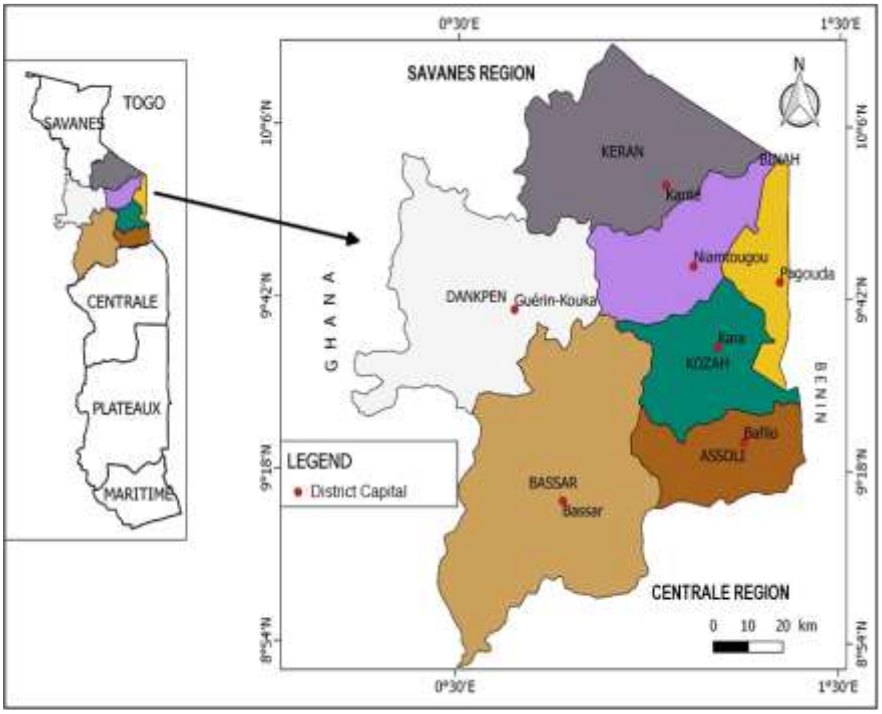

Fig-1: Location of the study area

The geographical coordinates are 9°40'0"N and 0°55'0"E in DMS (Degrees, Minutes and Seconds) or 9.66667 and 0.916667 (in decimal degrees). The altitude above sea level is 291 m. It houses a unique meteorological station where average temperature, humidity, dew point, pressure and visibility are measured.

Description of the data

For our application, we collected the monthly meteorological and astronomical data presented in Table 1.

Table 1.Collected parameters

Category	Variable	Unit	Type
Meteorological	Ambient Temperature	° C	Numeric
	Wind speed	$m.s^{-1}$	
Astronomical	Index of clarity	-	Numeric
	All sky insolation on a horizontal surface	$kWh.m^{-2}.d^{-1}$	
	Global solar	$W.m^{-2}.d^{-1}$	

ISSN: 2277-9655
Impact Factor: 5.164
CODEN: IJESS7

	irradiance		
	Global solar irradiation	$Wh.m^{-2}.d^{-1}$	

These time series are provided by MINESParisTech/Armines (France)[9]and the NASA-SSE database with a spatial resolution of 1° (approximately 100 km)[10]. They were collected over a period of 15 years, it means 180 months (1 January 1990 to 31 December 2004). NASA data is shown in Figure 3.

```
-BEGIN HEADER-
NASA/POWER SRB/FLASHFlux/MERRA2/GEOS 5.12.4 (FP-IT) 0.5 x 0.5 Degree Daily Averaged Data
Dates (month/day/year): 01/01/1990 through 12/31/2004
Location: Latitude  9.6667   Longitude 0.9167
Elevation from MERRA-2: Average for 1/2x1/2 degree lat/lon region = 233.93 meters   Site = na
Climate zone: na (reference Briggs et al: http://www.energycodes.gov)
Value for missing model data cannot be computed or out of model availability range: -999
Parameter(s):
ALLSKY_SFC_LW_DWN    SRB/FLASHFlux 1/2x1/2 Downward Thermal Infrared (Longwave) Radiative Flux (kW-hr/m^2/day)
CLRSKY_SFC_SW_DWN    SRB/FLASHFlux 1/2x1/2 Clear Sky Insolation Incident on a Horizontal Surface (kW-hr/m^2/day)
TS                   MERRA2 1/2x1/2 Earth Skin Temperature (C)
KT                   SRB/FLASHFlux 1/2x1/2 Insolation Clearness Index (dimensionless)
KT_CLEAR             SRB/FLASHFlux 1/2x1/2 Clear Sky Insolation Clearness Index (dimensionless)
YEAR MO DY ALLSKY_SFC_LW_DWN CLRSKY_SFC_SW_DWN     TS              KT         KT_CLEAR
-END HEADER-
1990 01 01           26.59           0.69           5.85           8.85           0.69
1990 01 02           26.09           0.67           5.85           8.40           0.67
1990 01 03           26.55           0.59           5.16           8.16           0.59
1990 01 04           27.04           0.68           5.84           8.14           0.68
1990 01 05           27.22           0.68           5.50           8.00           0.68
1990 01 06           27.84           0.65           5.71           8.57           0.65
1990 01 07           28.72           0.67           5.93           8.69           0.67
1990 01 08           27.31           0.58           5.05           8.16           0.58
1990 01 09           27.43           0.65           5.68           8.12           0.65
1990 01 10           26.43           0.58           5.09           8.77           0.58
1990 01 11           28.19           0.62           5.27           8.78           0.62
1990 01 12           29.66           0.59           5.25           8.05           0.59
1990 01 13           29.91           0.62           5.71           8.65           0.62
1990 01 14           28.43           0.60           4.76           8.29           0.60
1990 01 15           26.87           0.60           5.34           8.59           0.60
1990 01 16           28.51           0.63           5.61           8.46           0.63
1990 01 17           29.74           0.66           5.91           8.22           0.66
1990 01 18           29.75           0.66           5.97           8.13           0.66
1990 01 19           29.46           0.65           5.84           8.16           0.65
1990 01 20           30.11           0.66           5.84           8.13           0.66
1990 01 21           28.87           0.57           5.21           8.49           0.57
1990 01 22           27.38           0.63           5.59           8.73           0.63
1990 01 23           25.81           0.67           5.84           8.23           0.67
1990 01 24           25.02           0.65           5.69           8.80           0.65
1990 01 25           25.99           0.51           4.62           8.87           0.51
1990 01 26           26.47           0.53           4.89           8.44           0.53
1990 01 27           28.25           0.50           4.59           8.47           0.50
1990 01 28           28.27           0.50           4.54           8.31           0.50
```

Fig2. Overview of satellite data

Pretreatment of data

This step aims to homogenize the data before simulation. It consists in changing the starting formats: ISO for NASA and CSV for SODA in Excel single file format and then in Text (Separator: Tabulation) to meet the requirements of our working tool, Matlab.

Choice of parameters of the prediction model

The use of all input variables will be expensive in computing time. However, some parameters are dependent and strongly correlated with each other, so it is not necessary to use all input variables. In order to have a parsimonious model, we carried out an analysis of the correlation coefficients between the input variables (ambient temperature, wind speed, clarity index, all sky insolation and the global solar irradiation). To constitute

ISSN: 2277-9655
Impact Factor: 5.164
CODEN: IJESS7

the inputs of the neural network model, only a single variable is retained in a group of highly correlated variables. The results obtained are shown in Table 2.

Table 2. Autocorrelation matrix between input variables

	Ambient temperature	Wind speed	Clarity index	All sky Insolation	Solar irradiation
Ambient temperature	1				
Wind speed	-0.10	1			
Clarity index	0.28	0.06	1		
All sky Insolation	0.40	0.05	0.95	1	
Solar irradiation	0.30	0.02	0.67	0.67	1

According to Table 2, all sky insolation is highly correlated with solar irradiation; which eliminates all sky insolation. Also, the clarity index is very correlated with the solar irradiation. We can also eliminate solar irradiance. Table 3 provides an overview of the input variables selected.

Table 3.Overview of input variables

Ambient temperature	Wind speed	Clarity index
25.87	2.99	0.69
25.71	2.48	0.67
26.83	0.97	0.59

Normalization of parameters

In general, the databases undergo pretreatment, which consists in performing an appropriate normalization taking into account the amplitude of the values accepted by the network, before their use for the learning of the neural network; this to ensure a homogenization of the values propagated in the network.

The inputs and outputs are normalized between 0 and 1, with respect to their minimum or maximum value, by applying the normalization equation (1):

$$X_{normalized} = \frac{X - \min(X)}{\max(X) - \min(X)} \qquad (1)$$

where

- max (X): maximum values of the data represented as a vector X;
- min (X): minimum values of the data represented as a vector X.

This normalization ensures that one entry does not become preponderant to the detriment of others. The normalized values are shown in Table 4.

Table 4. Overview of Standard Input Variables

Ambient temperature	Wind speed	Clarity index
0.43138542	0.43880597	0.90540541
0.42087984	0.36268657	0.87837838
0.45830598	0.13731343	0.77027027

Analytical modeling of neural networks

An artificial neural network is a computational model whose original inspiration was a biological model, that is, the model of the human nervous brain. Artificial neural networks are optimized by statistical learning calculations. They are placed on the one hand, in the family of statistical applications, allowing to generate large functional, flexible and partially structured spaces, and on the other hand in the family of artificial intelligence methods, allowing decisions to be made relying more on perception than on formal logical reasoning [11].

ISSN: 2277-9655
Impact Factor: 5.164
CODEN: IJESS7

The mathematical model of an artificial neuron is illustrated in Figure 4. This neuron can be considered as an operator receiving a number of input variable from the external environment where other neurons, each of these inputs is weighted by a weight said synaptic weight, providing an output only when the sum exceeds an internal threshold. The evaluation of the output is typically done by the weighted sum of the inputs and the passage of these results through a non-linearity (a transfer function f) modeled by the equation (2)

$$y_i = \sum_{j=1}^{n} f(x_j w_{ij}) \qquad (2)$$

where :

- x_j is the component of the input vector;
- w_{ij} is the component of the synaptic weight vector and
- y_i is the desired output

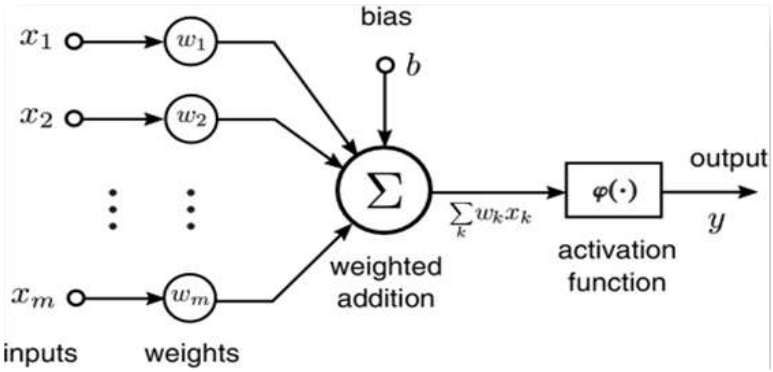

Figure 3.Structure of Artificial Neural Networks [12]

3. DEVELOPMENT OF A MODEL OF ARTIFICIAL NEURAL NETWORKS

It is in this part to simulate the Artificial Neural Networks parameters introduced using MatlabNN Tool utility.

Choice of Artificial Neural Networks Architecture

As we have output values (global solar radiation), we chose supervised learning, involving the Levenberg-Marquardt algorithm, which is a variation of the algorithm of the retro propagation of the gradient of the error. Indeed, it gives better results in terms of speed of convergence and generalization performance. Table 5 shows the configurations selected.

Table 5.Configurations retained

Configuration	Learning Algorithm	Input layer transfer function	Transfer function of the hidden layer neurons	Output layer transfer function
1	Levenberg -Marquardt	Purelin	Logsig	Purelin
2		Purelin	Purelin	Purelin
3		Purelin	Tansig	Purelin

Indeed, we opted for the Multilayer Perceptron because it meets the specificities of the prediction problem.
In our study, we have a Multilayer Perceptron network consisting of three (03) layer:

- an input layer, formed by three (03) neurons; these neurons represent the input variables: the clarity index, the wind speed and the ambient temperature; in this layer no calculation is made;
- a hidden layer, where all the optimization calculations of the parameters of the Artificial Neural Network are done;
- finally, an output layer which represents the daily average of solar radiation.

ISSN: 2277-9655
Impact Factor: 5.164
CODEN: IJESS7

In this work, we have adopted an approach which consists in considering first the simplest architecture (with a minimum of neurons in the hidden layer), then in making it more complex and in retaining the one which presents the best performances in randomly varying the number of hidden layers, the number of neurons in the hidden layer and the transfer functions.

Statistical analysis of models

For the validation of the models, the recourse is made to two (02) popular and widely used statistical indicators which are:

- the correlation coefficient (R), given by formula (3), it measures how much the predicted values are closer to the real values; clearly, a correlation coefficient value closer to unity implies a better prediction;

$$R = \left[\frac{\sum_{i=1}^{N} \left(G_{mes}(i) - \bar{G}_{mes}(i)\right) G_{mes}(i)}{\sqrt{\sum_{i=1}^{N} \left(G_{mes}(i) - \bar{G}_{mes}(i)\right)^2 \sum_{i=1}^{N} \left(G_{est}(i) - \bar{G}_{est}(i)\right)^2}} \right] \quad (3)$$

- the Root Mean Square Error (RMSE), estimated by formula (9); it identifies the precision comparing the difference between the values obtained during the estimation and those of the measured data, it always has a positive value;

$$RMSE = \left[\frac{1}{N} \sum_{i=1}^{N} \left(G_{mes}(i) - G_{est}(i)\right)^2 \right]^{1/2} \quad (4)$$

- ✓ N: number of examples used in the training or test database;
- ✓ Gmes: measured solar radiation ($Wh.m^{-2}.d^{-1}$);
- ✓ Gest: solar radiation estimated by the model ($Wh.m^{-2}.d^{-1}$);
- ✓ $\bar{G}$mes: average value of the measured solar radiation ($Wh.m^{-2}.d^{-1}$);
- ✓ $\bar{G}$est: average value of the estimated solar radiation ($Wh.m^{-2}.d^{-1}$);

4. RESULTS AND DISCUSSION

In this part, the simulation results of the artificial neural network parameters introduced are presented. The MatlabNN Tool utility is used for this purpose.

Learning phase

For configuration 1, the activation torque is Logsig - Purelin. The results are contained in Table 6. For this configuration, the best performance is obtained withthree (03) neurons in the hidden layer. R = 0.85 and RMSE=0.7.

Table 6. Performance of Configuration 1 (Logsig - Purelin)

Number of neurons in the hidden layer	MSE	RMSE	MAE	R^2	R
1	0.17	0.41	0.06	0.71	0.84
2	0.47	0.69	0.06	0.71	0.84
3	**0.49**	**0.70**	**0.06**	**0.72**	**0.85**
4	879.29	29.65	0.06	0.72	0.85
5	13.58	3.68	0.06	0.72	0.85
6	218.88	14.79	0.06	0.72	0.85
7	94.79	9.73	0.06	0.72	0.84
8	226.17	15.03	0.06	0.72	0.85
9	322.47	17.95	0.06	0.72	0.85

ISSN: 2277-9655
Impact Factor: 5.164
CODEN: IJESS7

10	79.36	8.90	0.06	0.72	0.84

Then, for configuration 2, the activation torque is Purelin - Purelin. The results are contained in Table 7. For this configuration, the best performance is obtained with two (02) neurons in the hidden layer. R = 0.84 and RMSE = 0.10.

Table 7. Performance of Configuration 2 (Purelin - Purelin)

Number of neurons in the hidden layer	MSE	RMSE	MAE	R^2	R
1	0.01	0.11	0.07	0.68	0.84
2	**0.01**	**0.10**	**0.07**	**0.68**	**0.84**
3	0.01	0.11	0.07	0.68	0.84
4	0.01	0.11	0.07	0.68	0.84
5	0.01	0.11	0.07	0.68	0.84
6	0.01	0.11	0.07	0.68	0.84
7	0.01	0.11	0.07	0.68	0.84
9	0.01	0.10	0.07	0.68	0.84
10	0.01	0.11	0.07	0.68	0.84

Finally, for configuration 3, the activation torque is Tansig - Purelin. The results are contained in Table 8. For this configuration, the best performance is obtained with three (03) neurons in the hidden layer. R = 0.85 and RMSE = 0.40.

Table 8. Performance of Configuration 3 (Tansig - Purelin)

Number of neurons in the hidden layer	MSE	RMSE	MAE	R^2	R
1	0.04	0.22	0.06	0.71	0.84
2	0 .12	0.35	0.06	0.71	0.84
3	**0.16**	**0.40**	**0.06**	**0.72**	**0.85**
4	0.24	0.49	0.06	0.72	0.85
5	0.35	0.59	0.06	0.72	0.85
6	49.57	7.04	0.06	0.72	0.85
7	4.16	2.04	0.06	0.72	0.85
8	101.98	10.09	0.06	0.72	0.85
9	171.54	13.09	0.06	0.72	0.85
10	1.10	1.05	0.06	0.72	0.84

After analysis, the best performance obtained for the three (03) configurations is presented in Table 9

Table 9.Characteristics of the best learning performance

Transfer function in the input layer	Transfer function in the output layer	Number of neurons in the hidden layer	R	RMSE
Tansig	Purelin	3	0,85	0,40

Note that the architecture with three (03) neurons in the hidden layer, a Tansig function for the input layer and a Purelin function for the output layer, gave the best performance with this algorithm.

Figure 5 shows the correlation between the predicted values and the measured values after learning.

ISSN: 2277-9655
Impact Factor: 5.164
CODEN: IJESS7

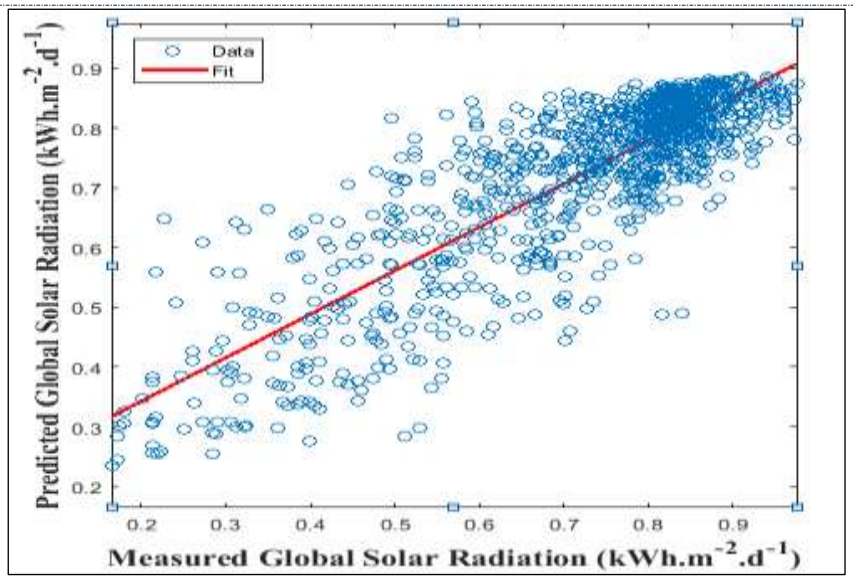

Figure 4.Correlation between target values and predicted values after data learning

The correlation coefficient which describes the approximation of the output (calculated global solar radiation value) of the target (measured overall solar radiation value) for the model chosen is R = 0.85 with and RMSE = 0.40.

Test and Validation Phase

The model adopted after learning is tested to determine its performance in predicting or generating synthetic daily data, by presenting it with a previously unused database (January 1, 2002 - December 31, 2004), different from those used for the first time learning. If the performances are not satisfactory, it will be necessary either to modify the architecture of the network, or to modify the base of learning. The correlation between the target values and the values predicted during the test is presented in Figure 6.

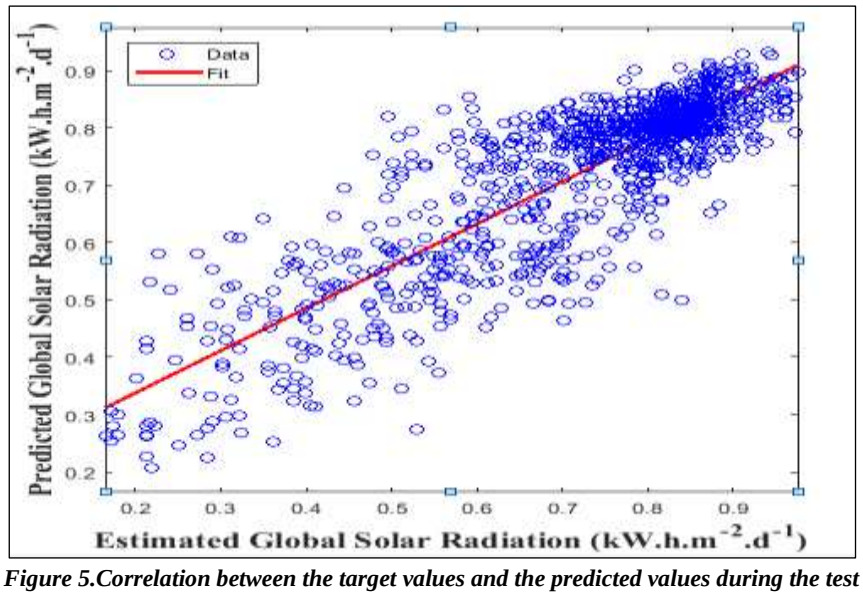

Figure 5.Correlation between the target values and the predicted values during the test

ISSN: 2277-9655
Impact Factor: 5.164
CODEN: IJESS7

The analysis in Figure 6 shows a regression line that represents the variation of the values predicted by the proposed model as a function of the actual values of the daily global solar radiation in the Kara region. Note that the correlation coefficient R = 0.85 and RMSE = 0.72.

The result of the prediction is shown in Figure 7. It shows the actual data of the daily averages of the global irradiation ($kWh.m^{-2}.d^{-1}$) as a function of time as well as their prediction calculated using the chosen model (Three-neuron multilayer perceptronin the hidden layer and a pair of Tansig-Purelin activation function).

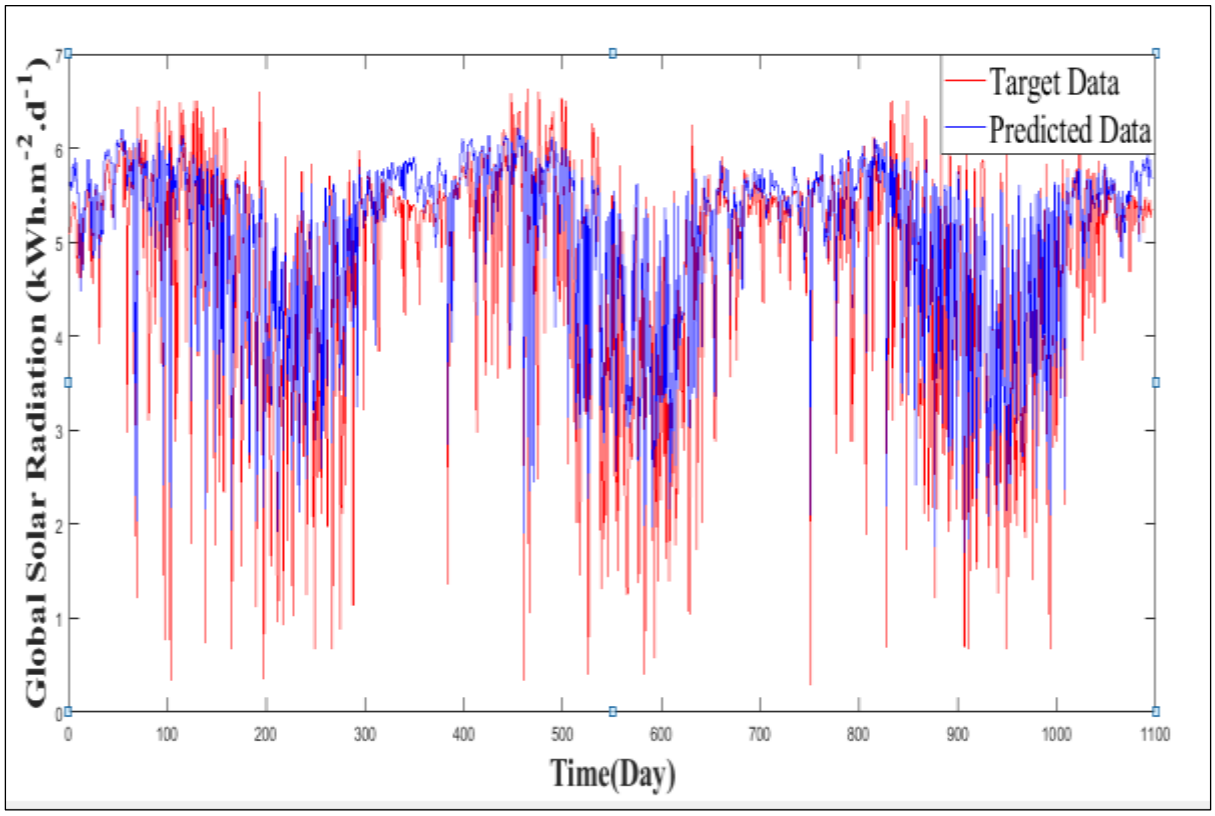

Figure 6.Comparative curves between target values and predicted values

The analysis of the figure reveals that the measurements of the global solar radiation coincide with the values calculated by the chosen model (three-neuron Multilayer Perceptron in the hidden layer and a pair of Tansig-Purelin activation function. It can be deduced that the proposed model generates the global daily radiation of the Kara region in a satisfactory manner. However, it appears that the quality (accuracy) of prediction depends on the time of year. Nevertheless, data collected over a longer period could have helped us to perfect our results.

5. CONCLUSION

The model designed in this work for the prediction of solar potential in Kara region is a Multilayer Perceptron. The best performances are obtained with three (03) neurons in the hidden layer and a couple of activation function (Tansig - Purelin).

In sum, the use of neural networks for the prediction of global solar radiation at the Kara site has allowed us to obtain a good prediction result because the target values are very close to the values predicted by the model.

Indeed, for this model we observe R = 0.85 and RMSE = 0.40 between the measured data and those estimated; which validates the use of this model for the purpose of predictions. Finally, the simulation of the predicted data

ISSN: 2277-9655
Impact Factor: 5.164
CODEN: IJESS7

with this model gives a daily mean irradiation of 5.0255 $kWh.m^{-2}.d^{-1}$ then against 4.7366 $kWh.m^{-2}.d^{-1}$ measured by NASA and therefore relative error of 5.7486%,. It implies a slight overestimation of 0.2889 $kWh.m^{-2}.d^{-1}$.

This leads us to say that these models can be used to estimate global solar radiation for places with climates similar to those of this site provided that the data is considerable.

This work, although partial, is a step towards a better understanding of the predictive analysis of global solar radiation data in Kara region. However, they can be improved.

Thus, as a perspective in our study we envisage: increasing the size of the data in the database, using other types of neural networks for the prediction of global solar radiation, or hybrid methods for example between genetic algorithms, wavelet networks, or fuzzy logic, take into account the inclination and orientation of PV modules in order to provide a practical estimate of solar potential.

REFERENCES

[1] Fatiha Trahi, Prédiction de l'irradiation solaire globalepour la région de Tizi – Ouzou par lesréseaux de neurones artificiels : application pour le dimensionnement d'une installation, photovoltaïque pour l'alimentation du laboratoire de recherche LAMPA, Thesis of Magister in Electronics, Option: Remotesensing. University of Mouloud Mammeri of Tizi-Ouzou, 2011.
[2] CyrilVoyant, Prédiction de séries temporelles de rayonnement solaire global et de production d'énergie photovoltaïque à partir de réseaux de neurones artificiel, Thesis for obtaining the degree of Doctor in Physics, Mention: Energetics, University of Corse-Pascal Paoli, 2011.
[3] Hanae LOUTFI, Prédiction des composantes de l'irradiation solaire horaire sur plan horizontal en utilisant les réseaux de neurones artificiels, Thesis for obtaining the State Doctorate, Discipline: Physics, Speciality: Energetic. University Mohammed V, Oct 2017.
[4] F.S. Tymvios,C.P. Jacovides, S.C. Michaelides, C. Scouteli, Comparative study of Angstroms and artificial neural networks methodologies in estimating global solar radiation, Solar Energy 78, 752-762.
[5] YingniJiang, Computing of monthly mean dailyglobal solar radiation in China using artificialneural networks and other empirical models ", Energy 34, pp.1276-1283, Sept2009.
[6] KomlanAmegassivi (2012), "Maîtrise de l'énergie auTogo", Master thesis MBA, Enseignement Supérieur d'Ingénierie Appliquée à la Thermique, l'Energie et l'Environnement.
[7] https://forumpresidentieldelajeunesse.com/les-5-regions/region-de-kara/potentialites/,accessed on 12/30/2018.
[8] Direction Générale de la Statistique et de la Comptabilité Nationale de la République du Togo, Rapport 2012.
[9] https://www.soda-pro.com/webservice/meteodata, accessed on 11/15/18
[10] https://www.power.larc.nasa.gov,accessed 11/13/18
[11] AMellit, S. A. Kalogirou, L. Hontoria, S.Shaari, "Artificial intelligence techniques for sizing photovoltaic systems", Renewable and Sustainable Energy Reviews, Vol 13, pp. 406-419, Feb 2008.
[12] Bhavin J.Shastri, Alexander N. Tait, Thomas Ferreira de Lima, Mitchell A. Nahmias, Hsuan-Tung Pengand Paul R. Prucnal, Neuromorphic Photonics, "Principles of, Encyclopedia of Complexity and Systems Sciences", Dec 2017.